RESEARCH ARTICLE
ISSN 2472-1972

Hormonal Regulation of Autophagy in Thyroid PCCL3 Cells and the Thyroids of Male Mice

Tomomi Kurashige,[1] Yasuyo Nakajima,[2] Mika Shimamura,[1] Masanobu Yamada,[2] and Yuji Nagayama[1]

[1]Department of Molecular Medicine, Atomic Bomb Disease Institute, Nagasaki University, Nagasaki, 852-8523, Japan; and [2]Department of Internal Medicine, Division of Endocrinology and Metabolism, Gunma University Graduate School of Medicine, Maebashi, 371-8511, Japan

ORCiD numbers: 0000-0002-5216-5785 (T. Kurashige); 0000-0003-2630-2579 (Y. Nakajima); 0000-0002-3830-2173 (M. Shimamura); 0000-0003-4426-2670 (M. Yamada); 0000-0002-5058-9349 (Y. Nagayama).

Autophagy is an evolutionarily conserved catabolic process by which cells degrade intracellular proteins and organelles in the lysosomes and recycle their metabolites. We have recently demonstrated the crucial role for the basal level of autophagic activity in thyrocyte survival and homeostasis using the thyroid-specific autophagy knockout mice. Here, we first studied hormonal regulation of autophagy in thyrocytes in vitro using a rat thyroid cell line PCCl3 and in vivo with mice. In cultured PCCl3 cells, thyroxine decreased microtubule-associated protein 1 light chain 3 (LC3) puncta (a component of autophagosome) and increased p62 (an autophagy substrate) levels, showing thyroxine-suppression of autophagy. In contrast, TSH increased both LC3 puncta and p62 levels, but at the same time stabilized p62 protein by inhibiting p62 degradation, indicating TSH induction of autophagy. Our experiments with various inhibitors identified that both the cAMP-protein kinase (PK) A-cAMP response element binding protein/ERK and PKC signaling pathways regulates positively autophagic activity. The in vivo results obtained with wild-type mice treated with methimazole and perchlorate or thyroxine were consistent with in vitro results. Next, in thyroid-specific autophagy knockout mice treated with methimazole and perchlorate (that is, mice were placed under a stressed condition where enhanced autophagy was required) for 2 months, lower follicle sizes and lower thyroglobulin contents in thyrocytes were observed, suggesting impaired thyroglobulin production presumably from insufficient nutrient supply. We therefore conclude that TSH positively regulates autophagic activity through the cAMP-PKA-cAMP response element binding protein/ERK and PKC signaling pathways, whereas thyroid hormones inhibit its activity in thyrocytes. Metabolites produced by autophagy appear to be necessary for protein synthesis stimulated by TSH.

Key Words: thyroid, autophagy, thyrotropin, thyroid hormone, ATG5

Autophagy is an evolutionarily conserved catabolic process by which cells degrade intracellular proteins and organelles in the lysosomes and recycle their metabolites. Autophagy occurs at basal levels constitutively and digests the damaged and superfluous proteins/organelles, and is also induced under various stress conditions, such as starvation, to supply

Abbreviations: 8-OHdG, 8-hydroxy-2′-deoxyguanosine; ATG, autophagy-related protein; CREB, cAMP response element binding protein; DMSO, dimethyl sulfoxide; H&E, hematoxylin and eosin; HRP, horseradish peroxidase; IF, immunofluorescence; LC3, microtubule-associated protein 1 light chain 3; KO, knockout; LAMP1, lysosomal-associated membrane protein 1; PKA, protein kinase A; PKC, protein kinase C; ROS, reactive oxygen species; TG, thyroglobulin; TH, thyroid hormone; WT, wild-type.

Received 20 November 2019
Accepted 7 May 2020
First Published Online 15 May 2020
Corrected and Typeset 9 July 2020

energy to the ells [1]. We have recently studied the consequence of thyroid-specific defect of autophagy-related protein 5 (ATG5), a critical component of autophagic machinery, on thyroid morphology and function in mice and found accumulation of ubiquitin-conjugated aggregated proteins, increased intracellular reactive oxygen species (ROS) and apoptotic death of thyrocytes, demonstrating the crucial role for the basal level of autophagic activity in thyrocyte survival and homeostasis [2].

Autophagy has been shown to play roles in the pathophysiology of various thyroid diseases. For instance, autophagy has been reported to play a role in pathogenesis of Graves' orbitopathy by inducing differentiation of fibroblasts into adipocytes and accumulation of adipose tissues [3]; inhibition of autophagy (and elevation of ROS) by proinflammatory cytokines (IL-1β and interferon-γ and IL-23) and iodine has been proposed to be attributed to the pathogenesis of Hashimoto thyroiditis [4-6]; polybrominated diphenyl ether-47, a flame retardant and a developmental neurotoxicant, has shown to cause thyroid toxicity [7]; and defective autophagy in young rats has been associated with radiation-induced thyroid carcinogenesis [8]. Autophagy has also been extensively studied as a therapeutic target in thyroid cancer field [9], but the data are controversial with some papers showing pro-survival [10, 11] but others anti-survival effects of autophagy on thyroid cancers [12, 13].

However, regulation of autophagy in thyrocytes by hormones such as TSH and thyroid hormone (TH) has not been studied. We found 1 paper reporting TSH suppression of autophagy in chondrocytes [14], and several papers showing TH enhancement of autophagy in different types of mammalian cells, such as liver, muscle, and fat cells [15-17]. Hormonal regulation of autophagy has also been recently examined in various organs, such as Sertoli cells by testosterone, liver by growth hormone, and skeletal muscle by insulin (ref. [15] and references therein).

Here, we first studied hormonal regulation of autophagy in thyrocytes in vitro using a rat thyroid cell line PCCl3 and in vivo with mice. Having found the positive regulation of autophagy by TSH, we further evaluated the significance of TSH-induced autophagy in the thyroid homeostasis in thyroid-specific autophagy knockout (KO) mice.

1. Materials and Methods

A. In vitro experiments

A normal differentiated rat thyroid cell line PCCl3 [18] was cultured in Coon's modified F-12 medium supplemented with 5% fetal bovine serum; TSH, insulin, and transferrin; and antibiotics as previously described [19]. To evaluate the effects of TSH, T4 and 8-Br-cAMP on autophagic activity, the cells were first incubated without 2H (insulin and transferrin) for 3 days, and then stimulated with various doses of TSH (catalog no. T8931-1VL, Sigma-Aldrich, St Louis, MO; dissolved in PBS; the stock solution, 1 U/mL) in the presence/absence of staurosporine (catalog no. 197-10251, FUJIFILM Wako, Osaka, Japan; dissolved in dimethyl sulfoxide (DMSO); the stock solution, 100 μM), T4 (catalog no. T1775, Sigma-Aldrich; dissolved in water; the stock solution, 20 μg/mL), or 8-Br-cAMP (catalog no. 1140, TOCRIS Bioscience, Bristol, UK; dissolved in DMSO; the stock solution, 100 mM) for 24 hours. The effects of rapamycin (catalog no. tlrl-rap, InvivoGen, San Diego, CA; dissolved in DMSO; the stock solution, 10 mM) and chloroquine (catalog no. 08660-04, NACALAI TESQUE, Kyoto, Japan; dissolved in PBS; the stock solution, 10 mM) were examined in the cells cultured in the presence of TSH, insulin, and transferrin. The effects of KT5720 (catalog no. 420320, Merck KGaA, Darmstadt, Germany; dissolved in DMSO; the stock solution, 2 mM), 666-15 (catalog no. 538341, Sigma-Aldrich; dissolved in DMSO; the stock solution, 10 mM), U0126 (catalog no. V112A, Promega, Madison, WI; dissolved in DMSO; the stock solution, 10 mM), and cycloheximide (catalog no. C7698, Sigma-Aldrich; dissolved in DMSO; the stock solution, 1 M) were examined in the cells cultured in the presence of 8-bromo-cAMP (100 μM), 2H (insulin and transferrin) and fetal bovine serum.

In vivo experiments

Atg5^{flox}, *TPO-Cre* and *Atg5*$^{flox/flox}$;*TPO-Cre* mice (*Atg5*$^{thyr\text{-}KO/KO}$) mice were described previously [2].

Eight-week-old wild-type (WT) male C57BL/6J mice (Charles River Japan, Yokohama, Japan) were left untreated or treated with M/P (both 0.05%) or T4 (0.5%) in the drinking water for 2 weeks (n = 3 for each group), or 4-week-old *Atg5*$^{thyr\text{-}KO/KO}$ and littermate WT male C57BL/6J mice were left untreated or treated with M/P or T4 in the drinking water for 8 weeks (n = 4). Mice were then anesthetized with isoflurane, from which blood samples were collected via cardiac tap for serum preparation, and then euthanized by cervical dislocation. The thyroids were removed for histological examinations, and blood samples were used to measure TSH and T4 concentrations.

All mice were kept in a specific pathogen-free facility. Animal care and all experimental procedures were performed in accordance with the Guideline for Animal Experimentation of Nagasaki University with approval of the Institutional Animal Care and Use Committee (permission #1309021089). All surgeries were performed under isoflurane anesthesia and all efforts were made to minimize suffering.

B. Serum TSH and T4 measurements

Serum TSH was measured in a single assay by in-house mouse TSH RIA with the standard hormone (mouse TSH/LH reference; AFP9090D), antiserum (mouse TSH antiserum; AFP98991) [20], and the labeling hormone (rat TSH; NIDDK-rTSH-I-9), all of which were obtained from Dr. Parlow AF (Harbor-UCLA Medical Center, Torrance, CA). The lower detection limit was 1.25 ng/mL. Serum T_4 was measured in a single assay with commercially available mouse T4/thyroxine ELISA Kit (LS-F10014, LifeSpan BioSciences, WA) with the OD value of each well determined using a microplate reader (2030 Multilabel Plate Reader ARVO X3, PerkinElmer, Branchburg, NJ) set to 450 nm.

C. Hematoxylin and eosin and immunofluorescence staining of tissues

The thyroids were fixed in 10% neutral-buffered formalin or Bouin solution (023-17361, FUJIFILM Wako, for 8-hydroxy-2′-deoxyguanosine [8-OHdG]) and then embedded in paraffin. Four-micrometer-thick sections were prepared and hematoxylin and eosin (H&E)-stained or immune-stained. The specimens were deparaffinized and subjected to antigen retrieval by microwave treatment in 10 mM citrate buffer (pH 6), followed by primary and secondary antibody incubation. The primary and secondary antibodies used were (i) guinea pig polyclonal anti-p62 (catalog no. GP62-C, Progen, Heidelberg, Germany; 1:100 dilution) [21] and Alexa Fluor 488-conjugated goat polyclonal anti-guinea pig IgG (catalog no. ab150185, Abcam, Cambridge, UK; 1:200 dilution) [22] for p62; (ii) rabbit polyclonal anti-LC3 (catalog no. PM036, Medical & Biological Laboratories, Nagoya, Japan; 1:1,000 dilution) [23] and Alexa Fluor 488-conjugated goat polyclonal anti-rabbit IgG (catalog no. A-11008, Life Technologies, Tokyo, Japan; 1:200 dilution) [24] for LC3; (iii) rabbit polyclonal anti-ubiquitin (catalog no. ADI-SPA-200-D, ENZO, Farmingdale, NY; 1:50 dilution) [25] and Alexa Fluor 488-conjugated goat polyclonal anti-rabbit IgG (catalog no. A-11008, Life Technologies; 1:200 dilution) [24] for ubiquitin; (iv) rabbit anti-53BP1 (catalog no. A300-272A, Bethyl, Montgomery, TX; 1:200 dilution) [26] and Alexa Fluor 488-conjugated goat polyclonal anti-rabbit IgG (catalog no. A-11008, Life Technologies; 1:200 dilution) [24] for 53BP1; (v) mouse monoclonal anti 8-OHdG (clone no. N45.1, catalog no. MOG-020P, Japan Institute for the Control of Aging, Shizuoka, Japan; 1:10 dilution) [27] and Alexa Fluor 488-conjugated goat polyclonal anti-mouse IgG (catalog no. A-11001, Life Technologies; 1:200 dilution) [28] for 8-OHdG; (vi) rabbit monoclonal anti-TG (clone no. EPR973, catalog no. ab 156008, Abcam; 1:250 dilution) [29] and Alexa Fluor 488-conjugated goat polyclonal anti-rabbit IgG (catalog no. A-11008, Life Technologies; 1:200 dilution) [24] for thyroglobulin

(TG); and (vii) rabbit polyclonal anti-lysosomal-associated membrane protein 1 (LAMP1; ab24170, Abcam; 1:500 dilution) [30] and Alexa Fluor 594-conjugated goat polyclonal anti-rabbit IgG (A11012, Life Technologies; 1:200 dilution) [31] for LAMP1. The staining without the primary antibodies was performed as negative controls in all experiments. Incubation times were 60 minutes for primary antibodies and 30 minutes for secondary antibodies, both at room temperature. The slides were analyzed using an All-in-One BZ-9000 Fluorescence Microscope (Keyence, Osaka, Japan) and the fluorescent intensity was quantified using a BZ-II Analyzer (Keyence). One hundred cells were evaluated in each sample to measure the fluorescent intensities of p62, ubiquitin, and 8-OHdG, and number of LC3 puncta and 53BP1 foci.

D. Immunofluorescence staining of cells

The cells were fixed with 3.7% formaldehyde for 10 minutes, permeabilized with 0.1% Triton-X. The primary and secondary antibodies used for p62 and LC3 were described previously. The cells were then embedded with VECTASHIELD Mounting Medium containing DAPI (Vector Laboratories, Burlingame, CA). The slides were analyzed using an All-in-One BZ-9000 Fluorescence Microscope (Keyence), and the fluorescent intensity was quantified using a BZ-II Analyzer (Keyence). Fifty cells were evaluated in each sample to measure the fluorescent intensities of p62 and the number of LC3 puncta.

E. Western blotting

Expression of LC3 and p62 was also determined by immunoblotting with 40 μg of thyroid tissues lysate prepared with PCCl3 cells, as described previously [2]. The primary and secondary antibodies used were (i) polyclonal rabbit anti-LC3 (catalog no. PM036, Medical & Biological Laboratories; 1:1000 dilution) [23] and polyclonal goat anti-rabbit horseradish peroxidase (HRP)-conjugated IgG (catalog no. 7074, Cell Signaling Technology, Danvers, MA; 1:1000 dilution) [32] for LC3; (ii) polyclonal guinea pig anti-p62 (catalog no. GP62-C, Progen; 1:1000 dilution) [21] and polyclonal rabbit anti-guinea pig HRP-conjugated IgG (catalog no. 61-4620, Innovative Research, Novi, MI; 1:1000 dilution) [33] for p62; and (iii) monoclonal mouse anti β-actin (clone no. C4, catalog no. sc-47778, Santa Cruz Biotechnology, Dallas, TX; 1:1000 dilution) [34] and polyclonal horse anti-mouse HRP-conjugated IgG (catalog no. 7076, Cell Signaling Technology; 1:1000 dilution) [35] for β-actin.

F. Quantitative real-time PCR

Total RNA was extracted from PCCl3 cells treated with/without TSH (10 mU/mL) for 24 hours using ISOGEN reagent (Nippon Gene, Tokyo, Japan). cDNA was synthesized from 500 ng total RNA with SuperScript III reverse transcriptase (Thermo Fisher Scientific, Waltham, MA) using random hexamers. Quantitative PCR was then carried out in a Thermal Cycler Dice Real-time system (Takara, Tokyo, Japan) using SYBR Premix EX Taq II (Takara). The primer pairs for p62 were 5′-ACGTGATTTGTGATGGTTGC-3′ and 5′-AGGACGTGGGCTCCAGTT-3′. The PCR condition was 40 cycles of denature at 95℃ for 15 seconds, annealing at 53℃ for 15 seconds, and extension at 72℃ for 20 seconds. The cycle threshold values, which were determined using a second derivative, were used to calculate the normalized expression of the indicated mRNAs using Q-Gene soft wave using β-actin for normalization. The negative control reaction was done without reverse transcription in parallel. The PCR product sizes were also confirmed with 2% agarose gel electrophoresis.

G. Statistical analyses

All data are expressed as mean ± SE and differences between groups were examined for statistical significance using the Dunnett's test. A P value < 0.05 was considered statistically significant. All the experiments were repeated at least twice with essentially the same results.

2. Results

A. Hormonal regulation of autophagic activity in PCCl3 cells

In this study, LC3 and p62 were used as biomarkers for monitoring autophagic flux as previously described [2]. As autophagy proceeds, LC3-I, ubiquitously expressed in the cytoplasm, is converted to LC3-II by lipidation and recruited to autophagosome. The amount of LC3-II can be monitored by western blotting showing the presence of a LC3-II band in addition to a LC3-I band (note that the molecular weight of LC3-II is higher than that of LC3-I [~18 kD] because of addition of lipid, but LC3-II migrates faster in gel because of high hydrophobicity and can be detected as an ~16 kDa band) and by immunofluorescence (IF) showing alteration of LC3 staining pattern from diffuse to punctate appearance. Furthermore, p62, a substrate of autophagy, is degraded in the autolysosome (fused autophagosome with lysosome). The amounts of p62 can be determined by western blotting and IF. Therefore, typically, increased LC3-II and decreased p62 indicate enhanced autophagic flux. However, increased LC3-II does not always mean higher autophagic activity but also inhibition of its autophagic degradation, because LC3-II itself is degraded in autophagy. For an example, chloroquine inhibits autophagy by suppressing the lysosomal function and thereby fusion of autophagosome and lysosome [36]; in this case, LC3-II is increased because the conversion of LC3-I to LC3-II is intact. Furthermore, the amount of p62 is reported to be regulated not only by autophagic degradation but also by transcriptional control [37-39]. Therefore, it is recommended to treat the cells with a reagent of your interest and an autophagic inhibitor, like chloroquine, which inhibits autophagy at the late step, to confirm its effect on autophagic flux [40].

We used a differentiated rat normal thyroid cell line PCCl3 to study the regulation of autophagy in vitro. The cells were first incubated with various doses of rapamycin (an mTOR inhibitor; because TOR is a well-known autophagy inhibitor, this chemical stimulates autophagic activity [41]) or chloroquine (an autophagy inhibitor; see previous section) for 24 hours. Rapamycin increased number of LC3 puncta and decreased p62 expression levels, and chloroquine increased both LC3 puncta and p62 levels dose-dependently in IF (Fig. 1A). The representative IF pictures are shown in Fig. 1B. These alterations were also confirmed by western blotting (Fig. 1C). Thus, these data confirm enhancement and inhibition by rapamycin and chloroquine, respectively, of autophagic activity, indicating that PCCl3 cells have functional autophagy.

Then, the effects of T4 and TSH on autophagy were evaluated in these cells. After incubation without any hormonal supplements for 3 days, the cells were incubated with different doses of T4 or TSH for 24 hours. T4 decreased LC3 puncta and increased p62 levels dose-dependently (Fig. 2A, left); the data can be simply interpreted as showing T4-suppression of autophagic activity, although the result is totally opposite to the mitophagy inducing action of T4 in nonthyroid mammalian cells such as skeletal muscle or adipocytes [15-17]. On the other hand, TSH increased both LC3 puncta and p62 expression (Fig. 2A, right), indicating either TSH inhibition of autophagy at the late step of autophagic flux (like chloroquine) or TSH stimulation of autophagy and of p62 levels as mentioned previously. However, it is very unlikely that TSH has a chloroquine-like lysosome-suppressive effect because the lysosome has the critical role in TSH stimulation of TH secretion from thyrocytes. Thus, TSH positively regulates endocytosis/pinocytosis of iodinated TG from the follicular lumen, forming colloid droplet/endosome, which then fuse with the lysosome. Thyroid hormones are then released from TG by proteolysis with lysosomal hydrolases and finally secreted into bloodstream [42]. Therefore, the cells were treated with rapamycin (a positive control) or TSH with chloroquine simultaneously as mentioned previously. As shown in Fig. 2B, increases in LC3 puncta by rapamycin or TSH were further increased by chloroquine. These data clearly indicate that TSH is an autophagy stimulator, not an inhibitor, and likely increases p62 levels independently from its action on autophagy. However, TSH increased the amount of p62 at posttranslational level, because TSH did not increase p62 mRNA levels in PCR

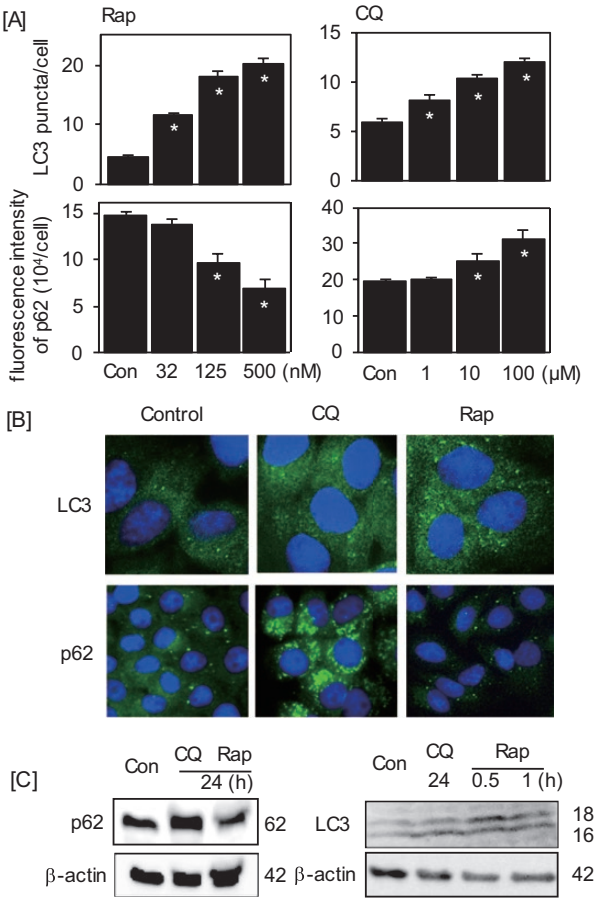

Figure 1. The effects of rapamycin and chloroquine on LC3 puncta/LC3-II and p62 levels in PCCl3 cells. The cells were incubated with the indicated doses of agents for 24 hours, or with 125 nM rapamycin for up to 2 hours. Expression of LC3 and p62 was determined by (A, B) IF staining or (C) western blotting, and expression levels were (A) quantified as described in the Materials and Methods. Con, control; CQ, chloroquine; LC3, microtubule-associated protein 1 light chain 3; Rap, rapamycin. Original magnifications: ×1000 for LC3 and ×400 for p62 in (C). Data are means ± SE. *$P < 0.01$ compared with control.

(Fig. 2C), but stabilized p62 protein in cycloheximide (a protein synthesis inhibitor)-treated cells (Fig. 2D). TSH stimulation of autophagic flux was also confirmed by colocalization experiments. Thus, simultaneous staining of p62 (a component of autophagosome; green) and LAMP1 (a lysosomal component; red) demonstrated colocalization of these 2 molecules (yellow-orange), indicating formation of autolysosome in TSH-stimulated cells, but this colocalization was abrogated by chloroquine (Fig. 2E). Overall, these data demonstrate that T4 suppresses, whereas TSH stimulates, autophagic activity, and additionally that TSH stabilizes p62 protein at posttranslational level.

Having found that TSH is an autophagy stimulator, we then focused on identifying TSH downstream signal pathways to control autophagic activity in PCCl3 cells. A cell membrane-permeable cAMP analog 8-Br-cAMP dose dependently increased LC3 puncta (Fig. 3A). TSH or 8-Br-cAMP mediated increases in LC3 puncta were dose dependently inhibited by a protein kinase A (PKA) inhibitor KT5720 (Fig. 3B) and to a slightly lesser extent by a protein kinase C (PKC) inhibitor staurosporine (Fig. 3C), thus demonstrating both Gs-cAMP-PKA and Gq-PKC being the stimulatory pathways for autophagy. Further downstream pathways were also studied with cAMP response element binding protein (CREB), ERK, and mTOR inhibitors. Both a CREB inhibitor 666-15 and an ERK inhibitor UO126, albeit to a lesser extent, declined 8-Br-CAMP-increase in LC3 puncta (Fig. 3D and 3E). Regarding rapamycin, although rapamycin itself clearly increased LC3 puncta (Fig. 1A), its effect on cAMP

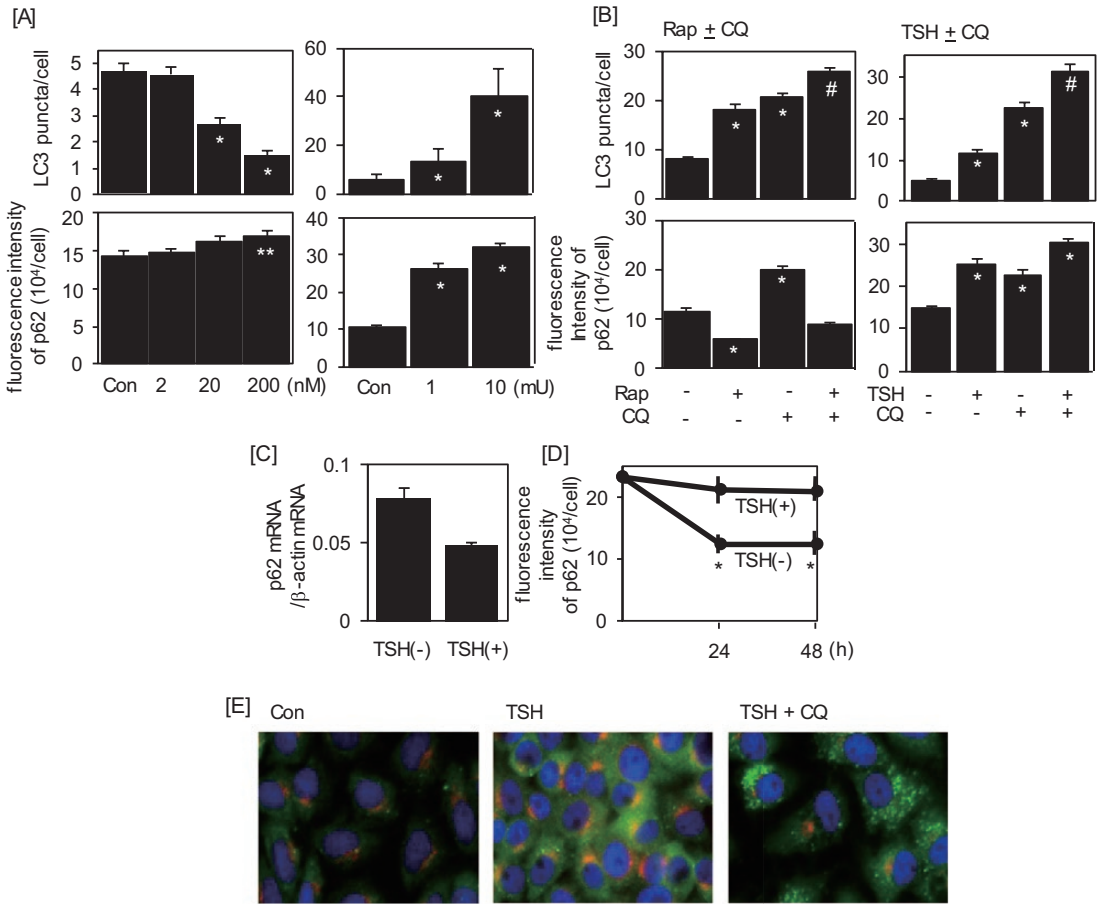

Figure 2. The effects of T4, TSH, chloroquine and/or rapamycin on autophagic activity, p62 mRNA/protein levels and colocalization of autophagosome and lysosome in PCCl3 cells. The cells were incubated with the indicated doses of (A) T4 or TSH or with (B) rapamycin (125 nM) or TSH (1 mU/mL) alone or in combination with chloroquine (10 μM) for 24 hours. (A, B) Expression of LC3 and p62 was determined by IF staining as described in the Materials and Methods. (C) Total RNA was extracted from the cells with/without TSH (1 mU/mL) for 24 hours and subjected to PCR. (D) Total cell lysates were prepared from the cells incubated in the presence of cycloheximide (12.5 μM) with/without TSH (1 mU/mL) for up to 48 hours, and subjected to quantification of p62 levels by IF. (E) The cells were incubated with TSH (1 mU/mL) alone or in combination with chloroquine (10 μM) for 24 hours and subjected to simultaneous staining of p62 and LAMP1. Con, control; CQ, chloroquine; IF, immunofluorescence; Rap, rapamycin. Data are means ± SE. $*P < 0.01$; $**P < 0.05$ compared with control; $\#P < 0.01$ compared with TSH or chloroquine alone.

increase in LC3 puncta was minimal (although significant) (Fig. 3F). These data are consistent with the previous report showing, under the basal level, mTOR remains active and keep a check on autophagy induction [43]. Altogether, both TSH-Gs-cAMP-PKA-CREB/ERK and TSH-Gq-PKC are signaling pathways to positively regulate autophagic activity, and autophagy inhibition by TSH-stimulated mTOR pathway appears minimal.

B. Hormonal regulation of autophagic activity in mice

Hormonal regulation of autophagy was also studied in mice. Mice were treated with rapamycin or chloroquine in the drinking water for 2 weeks. Neither thyroid histology (Fig. 4A), thyroid weights (Fig. 4B), nor T4 and TSH levels (Fig. 4C) were changed by these treatments, but increased LC3 puncta and decreased p62 levels were observed in rapamycin-treated mice, and increased LC3 puncta and p62 levels in chloroquine-treated mice (Fig. 4A and 4B),

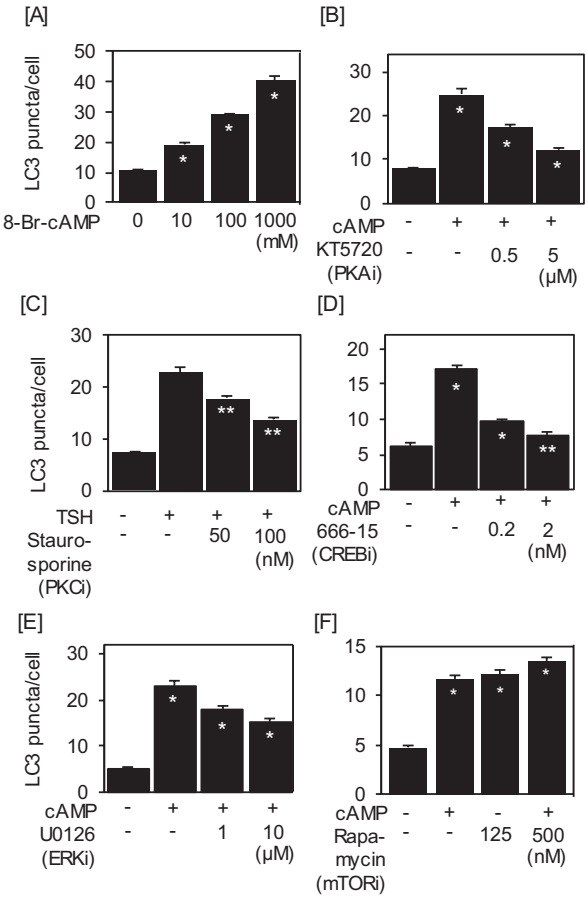

Figure 3. The effects of various inhibitors on TSH or 8-Br-cAMP induction of LC3 puncta in PCCl3 cells. The cells were incubated with TSH or 8-Br-cAMP alone or in combination with KT5720 (a PKA inhibitor), staurosporine (a PKC inhibitor), 666-15 (a CREB inhibitor), U0128 (an ERK inhibitor), or rapamycin (an mTOR inhibitor). LC3 puncta was determined by IF staining as described in the Materials and Methods. 8-OHdG, 8-hydroxy-2′-deoxyguanosine; CREB, cAMP response element binding protein; i, inhibitor; IF, immunofluorescence; PKA, protein kinase A; PKC, protein kinase C. Data are means ± SE. $*P < 0.01$; $**P < 0.05$ compared with control.

with data the same as those in PCCl3 cells (Fig. 1A). Mice were then treated with either methimazole and perchlorate or T4 in the drinking water for 2 weeks. Methimazole/perchlorate drastically changed thyroid histology (Fig. 4A), increased thyroid weights (Fig. 4B), and induced elevated TSH and suppressed T4 (Fig. 4C). Increased LC3 puncta and p62 levels were both observed in methimazole/perchlorate-treated mice (Fig. 4A and B). This is likely the net effect of enhancement of TSH increment in autophagic activity and p62 stabilization, and diminishment of T4 suppression of autophagic activity. By contrast, T4 treatment increased T4 levels but TSH remained unchanged (Fig. 4C). We could not explain why TSH was not suppressed, but the assay may possibly be less sensitive for lower TSH measurement. Instead, the lower epithelial heights in the thyroids of T4-treated mice than control mice (Fig. 4B) strongly indicated decreased TSH levels in the former. Supposing that TSH was suppressed, decreased LC3 puncta and p62 in T4-treated mice are likely attributed to the combined effect of TSH enhancement and T4 reduction of autophagic activity. Thus, these in vivo experiments using mice treated with either methimazole and perchlorate or T4 are consistent with the in vitro data mentioned previously.

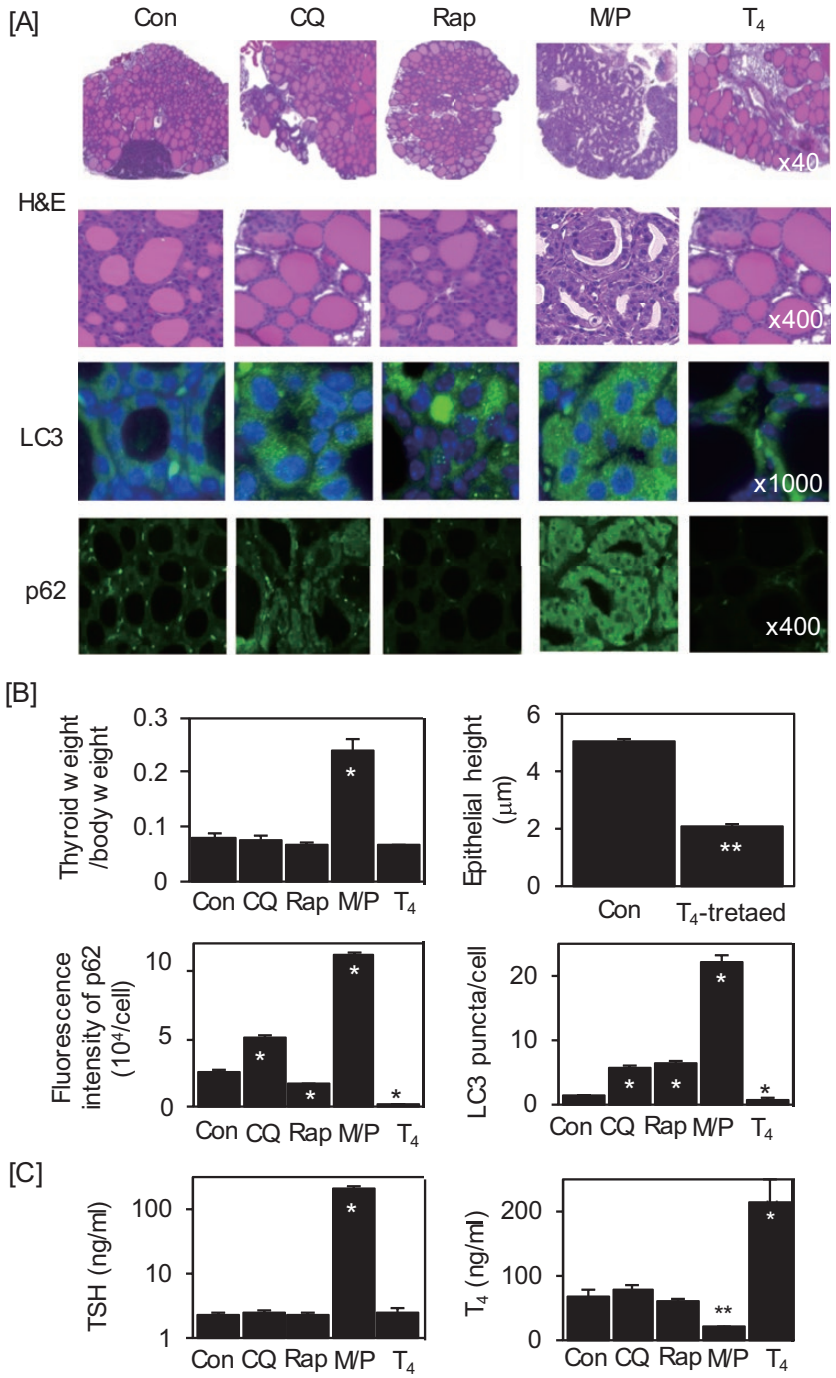

Figure 4. The effects of chloroquine, rapamycin, methimazole/perchlorate, and T4 on thyroid morphology, serum TSH and T4, LC3 puncta and p62 levels in WT mice. Mice were treated with these agents for 2 weeks; the thyroids were removed for weight measurement; (A) H&E and IHC for LC3 and p62; and (B) sera were obtained for TSH and T4 measurements as described in the Materials and Methods. Con, control; H&E, hematoxylin and eosin; LC3, microtubule-associated protein 1 light chain 3; M/P, methimazole and perchlorate; WT, wild-type. Original magnification, ×40-1000. Data are means ± SE. $*P < 0.01$; $*P < 0.05$ compared with control.

C. The effect of methimazole/perchlorate on thyroid homeostasis in autophagy KO mice

We have recently shown accumulation of ubiquitinated proteins and ROS-mediated DNA damages (8-OHdG) at 4 months, and decreased number of thyrocytes by apoptotic cell death and consequently decreased epithelial heights at 8 and 12 months in autophagy KO mice [2]. Slow progress of thyrocyte degeneration in these mice lacking the basal level of autophagy was somewhat unexpected, because the importance of autophagy is generally higher in nondividing cells [44], such as thyrocytes [45]. In an attempt to enhance the biochemical changes detected in 4-month-old mice and to accelerate the appearance of morphological changes observed in 8- to 12 month-old KO mice mentioned previously, enhanced autophagic activity was induced by feeding autophagy KO mice with methimazole/perchlorate for 2 months (between 2 and 4 months after birth). Methimazole/perchlorate enhanced accumulation of ubiquitinated proteins, ROS-mediated DNA damages (8-OHdG and 53BP1) and epithelial heights comparably in WT and KO mice (Fig. 5A–E); thus, our attempt failed. Instead, we found smaller follicular sizes, lower TG contents in thyrocytes (not follicle lumen) (Fig. 5A, 5F-5H) in methimazole/perchlorate-treated KO mice than in treated WT mice, implying lower TG production in methimazole/perchlorate-treated autophagy KO mice. These differences were not observed in mice treated with methimazole/perchlorate for a shorter period (2 weeks). Thus, enhanced production of TG (and probably also other proteins) by elevated TSH needs the metabolites generated and recycled by autophagy as building blocks.

3. Discussion

We here studied hormonal regulation of autophagy in thyrocytes in vitro and in vivo, and found that TSH positively regulates autophagic activity, whereas T4 has an opposite effect. The interpretation of the data on TSH regulation of autophagy is complicated, because TSH increased p62 expression levels, a marker for autophagic flux, independently from its action on autophagic activity. Although p62 expression is reported to be up-regulated at the transcription levels in certain conditions [37-39], our results indicate that TSH decreases the degradation rate of p62, meaning that TSH action is at posttranslational rather than transcriptional levels. As mentioned in the Introduction, TSH is reported to suppress autophagy (as demonstrated by reduced LC3-II and increased p62 levels) in chondrocytes by inhibiting phosphorylation of AMPK [14]. The detailed mechanisms for the differences in our data and theirs are at present unknown, but TSH action on autophagy appears to be cellular context dependent.

There are several papers reporting regulation of autophagy by intracellular signal transduction pathways. cAMP enhances autophagy in some papers [46, 47] but inhibits in others [48, 49] as do PKC [50, 51] and ERK [46, 52, 53]; CREB stimulates autophagy at transcriptional levels [54, 55]; and mTOR is indeed a well-known inhibitor of autophagy [41]. Our data demonstrate that the cAMP-PKA pathway and the further downstream signaling pathways involving CREB and ERK, and PKC pathway positively regulate autophagic activity in thyrocytes. ERK activation in thyrocytes involves both cAMP-dependent and cAMP-independent pathways [56]. By contrast, mTOR activation, mediated by the cAMP-PKA pathway, not by ERK or AKT in thyrocytes [57-59], has only a minimal negative effect on autophagy. As a result, it is concluded that TSH has the positive net effect on autophagic activity. Ugland et al. linked between cAMP induction of G1 cell-cycle arrest and enhanced autophagy in G1 arrest in mesenchymal stem cells [46], but this is not the case in thyrocytes, because the TSH-cAMP signal stimulates thyrocyte growth. Our data also indicate that CREB works at the downstream of the cAMP-PKA cascade in thyrocytes, while at the downstream of ERK in neural stem cells [55].

On the other hand, in contrast to other reports on many types of mammalian cells, T4 inhibits autophagic activity in thyrocytes. Although we did not scrutinize the molecular

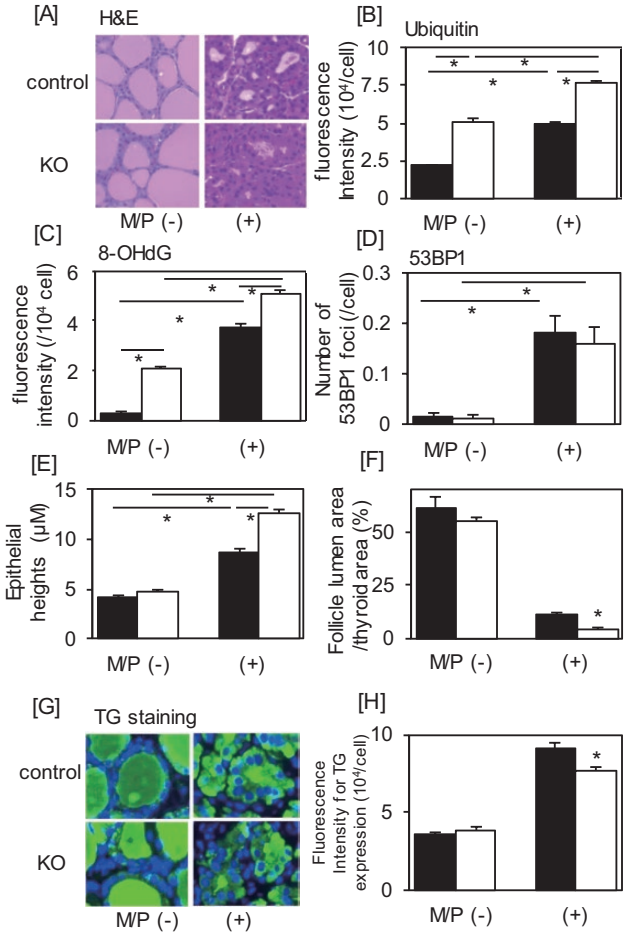

Figure 5. The effect of methimazole/perchlorate on the amounts of ubiquitin and DNA damages (53BP1 and 8-OHdG) in WT and autophagy KO mice. Eight-week-old WT and KO mice were left untreated or treated with methimazole/perchlorate in the drinking water for 2 months. The thyroids were then removed (A) for H&E, (E) measurements of epithelial heights and (B) IHC for ubiquitin, (C) 8-OHdG, (D) 53BP1, and (G, H) TG. Open and black bars indicate WT and KO mice, respectively. 8-OHdG, 8-hydroxy-2′-deoxyguanosine; H&E, hematoxylin and eosin; KO, knockout. Data are means ± SE. *$P < 0.01$ compared with control mice (B). Original magnification, ×400.

mechanisms for TH-inhibition of autophagy, it has been shown that T3 stimulated AMPK and inhibited mTOR in a ROS-dependent manner in muscle cells [15].

Finally, having found positive regulation of autophagy by methimazole and perchlorate, we treated autophagy KO mice with this chemical combination, that is, mice were placed under a stressed condition where enhanced autophagy was required. Smaller follicle sizes and lower TG contents in thyrocytes observed in these KO mice as compared with similarly treated wt mice imply that diminished nutrient supply because of a lack of autophagy may have caused lower TG production. In a situation where TSH increases synthesis of many proteins including TG, autophagy seems to play a critical role for sufficient building block supply.

It should also be noted here that an increment of 53BP1 foci by TSH, despite at its super-physiological levels, even in WT mice, demonstrating for the first time TSH induction of genomic double strand break.

In conclusion, we first demonstrate using PCCl3 cells that TSH positively regulates autophagic activity through the cAMP-PKA-CREB/ERK and PKC signaling pathways. Of interest, TSH increases expression level of p62, an autophagy substrate, at the

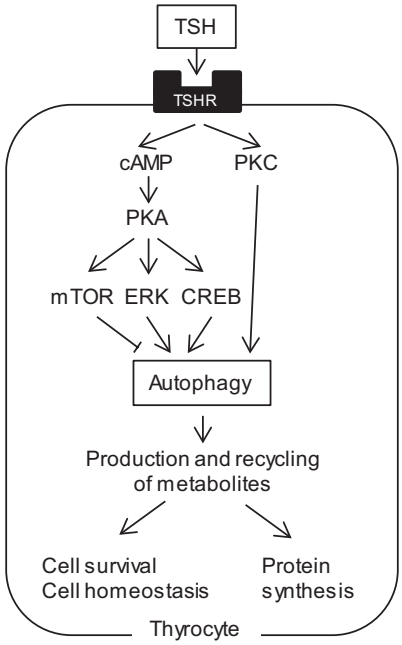

Figure 6. A scheme to summarize the functional significance of our previous and current studies in autophagic activity in thyrocyes. Autophagic activity is regulated positively by both cAMP and PKC signals, and in further downstream, positively by ERK and CREB but negatively by mTOR pathways. The metabolites produced by autophagy are recycled to keep cell homeostasis and survival at the steady state (2), and, when TSH is elevated, to supply building blocks for sufficient synthesis of proteins including TG stimulated by TSH. CREB, cAMP response element binding protein; PKC, protein kinase C.

posttranslational level, making interpretation of TSH action on autophagic activity difficult. In contrast, TH inhibits autophagy, the data totally opposite to TH action on autophagy in mammalian cells other than thyrocytes. Functionally, in vivo experiments reveal that, under a stressed condition where enhanced autophagy is required, recycling of metabolites generated by autophagy appear to be necessary for sufficient protein synthesis stimulated by TSH. The functional significance of our previous and current studies is summarized in Fig. 6.

Additional Information

Correspondence: Yuji Nagayama, MD/PhD, Department of Molecular Medicine, Atomic Bomb Disease Institute, Nagasaki University, 1-12-4 Sakamoto, Nagasaki 852-8523 Japan. E-mail: nagayama@nagasaki-u.ac.jp

Disclosure Summary: The authors also declare no conflict of interest.

Data Availability: All data generated or analyzed during this study are included in this published article or in the data repositories listed in References.

References and Notes

1. Ravanan P, Srikumar IF, Talwar P. Autophagy: the spotlight for cellular stress responses. *Life Sci.* 2017;**188**:53-67.
2. Kurashige T, Nakajima Y, Shimamura M, et al. Basal autophagy deficiency causes thyroid follicular epithelial cell death in mice. *Endocrinology.* 2019;**160**(9):2085-2092.
3. Yoon JS, Lee HJ, Chae MK, Lee EJ. Autophagy is involved in the initiation and progression of Graves' orbitopathy. *Thyroid.* 2015;**25**(4):445-454.

4. Lu Q, Luo X, Mao C, et al. Caveolin-1 regulates autophagy activity in thyroid follicular cells and is involved in Hashimoto's thyroiditis disease. *Endocr J*. 2018;**65**(9):893-901.
5. Zheng T, Xu C, Mao C, et al. Increased interleukin-23 in Hashimoto's thyroiditis disease induces autophagy suppression and reactive oxygen species accumulation. *Front Immunol*. 2018;**9**:96.
6. Xu C, Wu F, Mao C, et al. Excess iodine promotes apoptosis of thyroid follicular epithelial cells by inducing autophagy suppression and is associated with Hashimoto thyroiditis disease. *J Autoimmun*. 2016;**75**:50-57.
7. Li P, Liu L, Zhou G, et al. Perigestational exposure to low doses of PBDE-47 induces excessive ER stress, defective autophagy and the resultant apoptosis contributing to maternal thyroid toxicity. *Sci Total Environ*. 2018;**645**:363-371.
8. Matsuu-Matsuyama M, Shichijo K, Okaichi K, et al. Effect of age on the sensitivity of the rat thyroid gland to ionizing radiation. *J Radiat Res*. 2015;**56**(3):493-501.
9. Wei W, Hardin H, Luo QY. Targeting autophagy in thyroid cancers. *Endocr Relat Cancer*. 2019;**26**(4):R181-R194.
10. Yi H, Ye T, Ge M, et al. Inhibition of autophagy enhances the targeted therapeutic effect of sorafenib in thyroid cancer. *Oncol Rep*. 2018;**39**(2):711-720.
11. Wang W, Kang H, Zhao Y, et al. Targeting autophagy sensitizes braf-mutant thyroid cancer to vemurafenib. *J Clin Endocrinol Metab*. 2017;**102**(2):634-643.
12. Lin CI, Whang EE, Abramson MA, et al. Autophagy: a new target for advanced papillary thyroid cancer therapy. *Surgery*. 2009;**146**(6):1208-1214.
13. Xiang Y, Zhao J, Zhao M, Wang K. Allicin activates autophagic cell death to alleviate the malignant development of thyroid cancer. *Exp Ther Med*. 2018;**15**(4):3537-3543.
14. Xin W, Yu Y, Ma Y, et al. Thyroid-stimulating hormone stimulation downregulates autophagy and promotes apoptosis in chondrocytes. *Endocr J*. 2017;**64**(7):749-757.
15. Lesmana R, Sinha RA, Singh BK, et al. Thyroid hormone stimulation of autophagy is essential for mitochondrial biogenesis and activity in skeletal muscle. *Endocrinology*. 2016;**157**(1):23-38.
16. Sinha RA, Singh BK, Zhou J, et al. Thyroid hormone induction of mitochondrial activity is coupled to mitophagy via ROS-AMPK-ULK1 signaling. *Autophagy*. 2015;**11**(8):1341-1357.
17. Yau WW, Singh BK, Lesmana R, et al. Thyroid hormone (T3) stimulates brown adipose tissue activation via mitochondrial biogenesis and MTOR-mediated mitophagy. *Autophagy*. 2019;**15**(1):131-150.
18. *CVCL_6712*. https://web.expasy.org/cellosaurus/CVCL_6712.txt.
19. Kurashige T, Shimamura M, Nagayama Y. N-Acetyl-L-cysteine protects thyroid cells against DNA damage induced by external and internal irradiation. *Radiat Environ Biophys*. 2017;**56**(4):405-412.
20. *RRID:AB_2810234*, http://scicrunch.org/resolver/AB_2810234.
21. *RRID:AB_2687531*, http://scicrunch.org/resolver/AB_2687531.
22. *RRID:AB_2736871*, http://scicrunch.org/resolver/AB_2736871.
23. *RRID:AB_2274121*, http://scicrunch.org/resolver/AB_2274121.
24. *RRID:AB_143165*, http://scicrunch.org/resolver/AB_143165.
25. *RRID:AB_2039666*, http://scicrunch.org/resolver/AB_2039666.
26. *RRID:AB_185520*, http://scicrunch.org/resolver/AB_185520.
27. *RRID:AB_1106819*, http://scicrunch.org/resolver/AB_1106819.
28. *RRID:AB_2534069*, http://scicrunch.org/resolver/AB_2534069.
29. *RRID:AB_2814820*, http://scicrunch.org/resolver/AB_2814820.
30. *RRID:AB_775978*, http://scicrunch.org/resolver/AB_775978.
31. *RRID:AB_141359*, http://scicrunch.org/resolver/AB_141359.
32. *RRID:AB_2099233*, http://scicrunch.org/resolver/AB_2099233.
33. *RRID:AB_88247*, http://scicrunch.org/resolver/AB_88247.
34. *RRID:AB_2714189*, http://scicrunch.org/resolver/AB_2714189.
35. *RRID:AB_330924*, http://scicrunch.org/resolver/AB_330924.
36. Boya P, González-Polo RA, Casares N, et al. Inhibition of macroautophagy triggers apoptosis. *Mol Cell Biol*. 2005;**25**(3):1025-1040.
37. Nakaso K, Yoshimoto Y, Nakano T, et al. Transcriptional activation of p62/A170/ZIP during the formation of the aggregates: possible mechanisms and the role in Lewy body formation in Parkinson's disease. *Brain Res*. 2004;**1012**(1-2):42-51.
38. Fujita K, Maeda D, Xiao Q, Srinivasula SM. Nrf2-mediated induction of p62 controls Toll-like receptor-4-driven aggresome-like induced structure formation and autophagic degradation. *Proc Natl Acad Sci U S A*. 2011;**108**(4):1427-1432.

39. Trocoli A, Bensadoun P, Richard E, et al. p62/SQSTM1 upregulation constitutes a survival mechanism that occurs during granulocytic differentiation of acute myeloid leukemia cells. *Cell Death Differ*. 2014;**21**(12):1852-1861.
40. Mizushima N, Yoshimori T. How to interpret LC3 immunoblotting. *Autophagy*. 2007;**3**(6):542-545.
41. Díaz-Troya S, Pérez-Pérez ME, Florencio FJ, Crespo JL. The role of TOR in autophagy regulation from yeast to plants and mammals. *Autophagy*. 2008;**4**(7):851-865.
42. Braverman LE, Utiger RD. *Werner & Ingbar's the Thyroid*. Philadelphia: Lippincott Williams & Wilkens; 2000.
43. Noda T, Ohsumi Y. Tor, a phosphatidylinositol kinase homologue, controls autophagy in yeast. *J Biol Chem*. 1998;**273**(7):3963-3966.
44. Mizushima N, Levine B, Cuervo AM, Klionsky DJ. Autophagy fights disease through cellular self-digestion. *Nature*. 2008;**451**(7182):1069-1075.
45. Coclet J, Foureau F, Ketelbant P, Galand P, Dumont JE. Cell population kinetics in dog and human adult thyroid. *Clin Endocrinol (Oxf)*. 1989;**31**(6):655-665.
46. Ugland H, Naderi S, Brech A, Collas P, Blomhoff HK. cAMP induces autophagy via a novel pathway involving ERK, cyclin E and Beclin 1. *Autophagy*. 2011;**7**(10):1199-1211.
47. Zhang Y, Chen ML, Zhou Y, et al. Resveratrol improves hepatic steatosis by inducing autophagy through the cAMP signaling pathway. *Mol Nutr Food Res*. 2015;**59**(8):1443-1457.
48. Sarkar S, Ravikumar B, Floto RA, Rubinsztein DC. Rapamycin and mTOR-independent autophagy inducers ameliorate toxicity of polyglutamine-expanded huntingtin and related proteinopathies. *Cell Death Differ*. 2009;**16**(1):46-56.
49. Williams A, Sarkar S, Cuddon P, et al. Novel targets for Huntington's disease in an mTOR-independent autophagy pathway. *Nat Chem Biol*. 2008;**4**(5):295-305.
50. Xie Y, Kang R, Sun X, et al. Posttranslational modification of autophagy-related proteins in macroautophagy. *Autophagy*. 2015;**11**(1):28-45.
51. Zhang Y, Wu Y, Tashiro S, Onodera S, Ikejima T. Involvement of PKC signal pathways in oridonin-induced autophagy in HeLa cells: a protective mechanism against apoptosis. *Biochem Biophys Res Commun*. 2009;**378**(2):273-278.
52. Fan D, Liu SY, van Hasselt CA, et al. Estrogen receptor α induces prosurvival autophagy in papillary thyroid cancer via stimulating reactive oxygen species and extracellular signal regulated kinases. *J Clin Endocrinol Metab*. 2015;**100**(4):E561-E571.
53. Kinsey CG, Camolotto SA, Boespflug AM, et al. Protective autophagy elicited by RAF→MEK→ERK inhibition suggests a treatment strategy for RAS-driven cancers. *Nat Med*. 2019;**25**(4):620-627.
54. Seok S, Fu T, Choi SE, et al. Transcriptional regulation of autophagy by an FXR-CREB axis. *Nature*. 2014;**516**(7529):108-111.
55. Chong CM, Ke M, Tan Y, et al. Presenilin 1 deficiency suppresses autophagy in human neural stem cells through reducing gamma-secretase-independent ERK/CREB signaling. *Cell Death Differ*. 2018;**9**(9):879.
56. Vuchak LA, Tsygankova OM, Prendergast GV, Meinkoth JL. Protein kinase A and B-Raf mediate extracellular signal-regulated kinase activation by thyrotropin. *Mol Pharmacol*. 2009;**76**(5):1123-1129.
57. Blancquaert S, Wang L, Paternot S, et al. cAMP-dependent activation of mammalian target of rapamycin (mTOR) in thyroid cells. Implication in mitogenesis and activation of CDK4. *Mol Endocrinol*. 2010;**24**(7):1453-1468.
58. Malaguarnera R, Chen KY, Kim TY, et al. Switch in signaling control of mTORC1 activity after oncoprotein expression in thyroid cancer cell lines. *J Clin Endocrinol Metab*. 2014;**99**(10):E1976-E1987.
59. Cass LA, Meinkoth JL. Differential effects of cyclic adenosine 3',5'-monophosphate on p70 ribosomal S6 kinase. *Endocrinology*. 1998;**139**(4):1991-1998.